Epithelial-to-Mesenchymal Stem Cell Transition in a Human Organ: Lessons from Lichen Planopilaris

Hisayoshi Imanishi[1,2,12], David M. Ansell[1,12], Jérémy Chéret[3], Matthew Harries[1,4], Marta Bertolini[3,5], Norbert Sepp[6], Tamás Bíró[7], Enrique Poblet[8], Francisco Jimenez[9], Jonathan Hardman[1], Sreejith Parameswara Panicker[10], Christopher M. Ward[11] and Ralf Paus[1]

Epithelial-to-mesenchymal transition (EMT) is critical for embryonic development and wound healing, and occurs in fibrotic disease and carcinoma. Here, we show that EMT also occurs within the bulge, the epithelial stem cell (eSC) niche of human scalp hair follicles, during the inflammatory permanent alopecia, lichen planopilaris. We show that a molecular EMT signature can be experimentally induced in healthy human eSCs in situ by antagonizing E-cadherin, combined with transforming growth factor-β1, epidermal growth factor, and IFN-γ administration, which to our knowledge has not been reported previously. Moreover, induction of EMT within primary human eSCs can be prevented and even partially reversed ex vivo by peroxisome proliferator–activated receptor-γ agonists, likely through suppression of the transforming growth factor-β signaling pathway. Furthermore, we show that peroxisome proliferator–activated receptor-γ agonists also attenuates the EMT signature even in lesional lichen planopilaris hair follicles ex vivo. We introduce lichen planopilaris as a model disease for pathological EMT in human adult eSCs, report a preclinical assay for therapeutically manipulating eSC EMT within a healthy human (mini-)organ, and show that peroxisome proliferator–activated receptor-γ agonists are promising agents for suppressing and partially reversing EMT in human hair follicles eSCs ex vivo, including in lichen planopilaris.

Journal of Investigative Dermatology (2018) **138,** 511–519; doi:10.1016/j.jid.2017.09.047

INTRODUCTION

Epithelial-to-mesenchymal transition (EMT) is a physiological feature during embryogenesis and wound healing, but also occurs during pathological phenomena, such as the malignant transformation of epithelial cells, carcinoma metastasis, and several fibrotic diseases (Nieto et al., 2016; Stone et al., 2016). During EMT, epithelial cells gradually assume a fibroblast-like morphology as a result of transcriptional repression of E-cadherin via E-box binding factors, such as SNAI1 (SNAIL), SNAI2 (SLUG), and TWIST, and upregulation of mesenchymal hallmark proteins, such as vimentin and fibronectin (Nieto et al., 2016; Zeisberg and Neilson, 2009).

EMT is frequently investigated using immortalized cell lines that display an abnormal karyotype and epigenetic modifications not observed in normal cells (Serrano-Gomez et al., 2016). Primary cells are also utilized, even though these often adopt a wound healing–like spontaneous EMT response when cultured in vitro (Nieto et al., 2016; Stone et al., 2016). Therefore, the cellular behavior under these artificial conditions might not accurately reflect EMT as it occurs in vivo. Moreover, while existing animal models for studying EMT in vivo provide a native tissue environment, it is unclear how well these mimic human EMT under physiological or pathological conditions, or predict whether experimental therapies will translate to the clinic (Pasquier et al., 2015). This caveat is particularly relevant in the skin, given the many anatomical and functional differences between rodent and human skin. Finally, although EMT events can be studied in patient biopsies, these typically catch only the final stages in the stepwise and initially reversible EMT continuum (Nieto et al., 2016; Pasquier et al., 2015; Serrano-Gomez et al., 2016; Stone et al., 2016; Zeisberg and Neilson, 2009).

Therefore, clinically relevant models are urgently needed that permit one to study EMT initiation within human tissue in situ. It remains unknown whether adult epithelial stem cells (eSCs) undergo EMT in human skin and how this may relate to

[1]*Centre for Dermatology Research, University of Manchester, Manchester Academic Health Science Centre, National Institute for Health Research Biomedical Research Centre, Manchester, UK;* [2]*Department of Dermatology, Osaka City University Graduate School of Medicine, Japan;* [3]*Monasterium Laboratory, Münster, Germany;* [4]*Dermatology Centre, University of Manchester, Salford Royal NHS Foundation Trust, Salford, UK;* [5]*Department of Dermatology, University of Münster, Münster, Germany;* [6]*Department of Dermatology, Innsbruck Medical University, Innsbruck, Austria;* [7]*Departments of Immunology and Physiology, Faculty of Medicine, University of Debrecen, Debrecen, Hungary;* [8]*Department of Pathology, University General Hospital of Murcia, Murcia, Spain;* [9]*Mediteknia Dermatology Clinic, Medical Pathology Group, Instituto de Investigación Biosanitaria, Universidad de Las Palmas de Gran Canaria, Gran Canaria, Canary Islands, Spain;* [10]*Department of Zoology, University of Kerala, India; and* [11]*School of Dentistry, University of Manchester, Manchester, UK*

[12]*These authors contributed equally to this work.*

Correspondence: Ralf Paus, Centre for Dermatology Research, University of Manchester, Stopford Building, Oxford Road, Manchester, M13 9PT, UK. E-mail: ralf.paus@manchester.ac.uk

Abbreviations: AGED, N-Acetyl-GED; EMT, epithelial-to-mesenchymal transition; eSC, epithelial stem cell; HF, hair follicle; LPP, lichen planopilaris; PPAR, peroxisome proliferator–activated receptor; TGF, transforming growth factor

Received 2 May 2017; revised 15 September 2017; accepted 16 September 2017; accepted manuscript published online 26 October 2017; corrected proof published online 1 February 2018

fibrotic skin diseases. Human hair follicles (HFs) are a repository for eSCs (Purba et al., 2014) and show scarring hair loss (alopecia) when these eSCs get destroyed within their immunologically privileged niche, the bulge (Harries et al., 2013; Harries and Paus, 2010). Therefore, we aimed to explore whether human scalp HFs can serve as an instructive model system for studying the EMT process in eSCs in live human tissue.

For this, we focused on lichen planopilaris (LPP), one of the most frequently encountered primary cicatrial alopecias, a group of relatively rare, but clinically important inflammatory alopecias that result in skin scarring and permanent hair loss (Harries and Paus, 2010; Sinclair, 2016). While current evidence suggests that LPP results from a $CD8^+$ T-cell–driven attack on eSCs that have lost their relative immune privilege (Harries et al., 2013), the loss of eSCs alone does not explain the typically associated scarring. Indeed, when keratin 15+ve bulge eSCs were selectively deleted in mice, the resulting alopecia was not accompanied by scarring (Ito et al., 2005). However, abnormal expression of Snail has been identified in the fibrotic dermis of frontal fibrosing alopecia, another variant of primary cicatrial alopecia (Nakamura and Tokura, 2010), inviting the hypothesis that EMT may play a role in primary cicatrial alopecias (Nakamura and Tokura, 2011).

We have probed the working hypothesis that eSCs in the HF bulge undergo EMT in LPP and that this process may be experimentally induced even in healthy human bulge eSC ex vivo, if exposed to appropriate EMT-promoting stimuli. If confirmed, such an ex vivo assay should provide an excellent, clinically relevant model system for dissecting the as yet unclear molecular controls of human eSC EMT in situ, and for identifying candidate drugs that counteract eSC EMT under clinically relevant conditions. Here, we provide evidence in support of this working hypothesis by examining lesional LPP skin in situ and organ-cultured healthy human scalp HFs ex vivo.

RESULTS AND DISCUSSION

Lesional LPP HFs display morphological and ultrastructural signs of EMT within their epithelial stem cell niche

First, we re-examined our archive of LPP patient samples (Harries et al., 2013) and complemented this with biopsy material from additional LPP patients. Morphological analysis of the bulge compartment of lesional LPP HFs (as indicated by the arrector pili muscle insertion point [Figure 1a] and other previously defined human bulge markers [Purba et al., 2014]) revealed a breakdown of the usual, very tight segregation between the eSC compartment and the surrounding HF mesenchyme in lesional LPP HFs; occasionally even the highly pathological presence of spindled cells of myofibroblast-like appearance could be demonstrated within the bulge epithelium itself (Figure 1b).

These findings were followed by transmission electron microscopy. This confirmed the presence of fibroblastoid cells within lesional bulge epithelium and revealed putative collagen filaments within the cytoplasm of bulge keratinocytes (Figure 1c), a pathological ultrastructural phenomenon previously reported during EMT of ocular epithelium (Ogawa et al., 2009).

LPP bulge epithelium shows an mRNA and protein signature compatible with the occurrence of EMT

Next, we searched for aberrant expression of EMT-associated mRNA species in lesional bulge epithelium compared to non-lesion bulge areas from the same individual by quantitative real-time PCR (performed on mRNA that had previously been selectively obtained from the bulge by laser capture microdissection [Harries et al., 2013]). This approach elucidated the expression of several EMT-related genes in some of our LPP lesional biopsies, with no detectable expression in any non-lesional biopsy from the same patients. This was the case for *TWIST1* (2 of 6 patients), *ZEB2* (3 of 6 patients), *FN1* (fibronectin; 4 of 6 patients), *ACTA2* (α-smooth muscle actin; 4 of 6 patients), and *EMP1* (3 of 6 patients) (Supplementary Table S1 online). Other EMT-related transcripts were found in both the LPP lesional and non-lesional bulges, such as *CD44* (Supplementary Table S1), which is a known epithelial bulge marker (Szabo et al., 2013). More surprising was the presence of *SNAI2* and *ZEB1*, which might indicate that some (presumably reversible) EMT occurs long before clinical presentation. We did not observe an EMT signature in every single donor, which may reflect the severity of disease or the transient nature of EMT. However, the fact that we frequently detected EMT markers in LPP lesional bulge epithelium, but never in non-lesional bulge from the same donor adds weight to our hypothesis.

To more fully explore this, we assessed the protein expression of key EMT markers within the bulge of lesional LPP HFs compared to scalp from healthy volunteers via quantitative immunohistomorphometry (Harries et al., 2013) (Figure 1d and Supplementary Figure S1 online). This showed E-cadherin protein expression in the bulge of lesional LPP HFs to be significantly reduced, while the number of $vimentin^+$ or $fibronectin^+$ cells was significantly increased. When we also investigated the protein expression of early EMT markers, SNAIL protein–positive cells were significantly increased in the bulge epithelium of LPP, predominantly showing the expected nuclear immunoreactivity (Dubois-Marshall et al., 2011) (Supplementary Figure S1). Moreover, SLUG protein immunoreactivity was also significantly increased in LPP HFs, and a trend toward increased expression of TWIST protein was also observed (Figure 1c). Interestingly, SLUG protein was expressed predominantly within the cytoplasm, a phenomenon reported previously in Barrett's metaplasia (Jethwa et al., 2008) and ameloblastoma (Siar and Ng, 2014). ZEB1, α-smooth muscle actin, and CD44 protein expression did not differ significantly between lesional LPP and healthy control bulges (Supplementary Figure S2 online).

Cells undergoing EMT within the bulge express the eSC marker $keratin\ 15^+$

Next, we performed dual immunofluorescence microscopy of vimentin with the prototypic bulge SC marker, keratin 15 (Purba et al., 2014). This documented that at least some of the vimentin-expressing cells in the bulge of lesional LPP HFs represent eSCs (Figure 1e). These analyses also independently confirmed our previous finding that keratin 15 is markedly

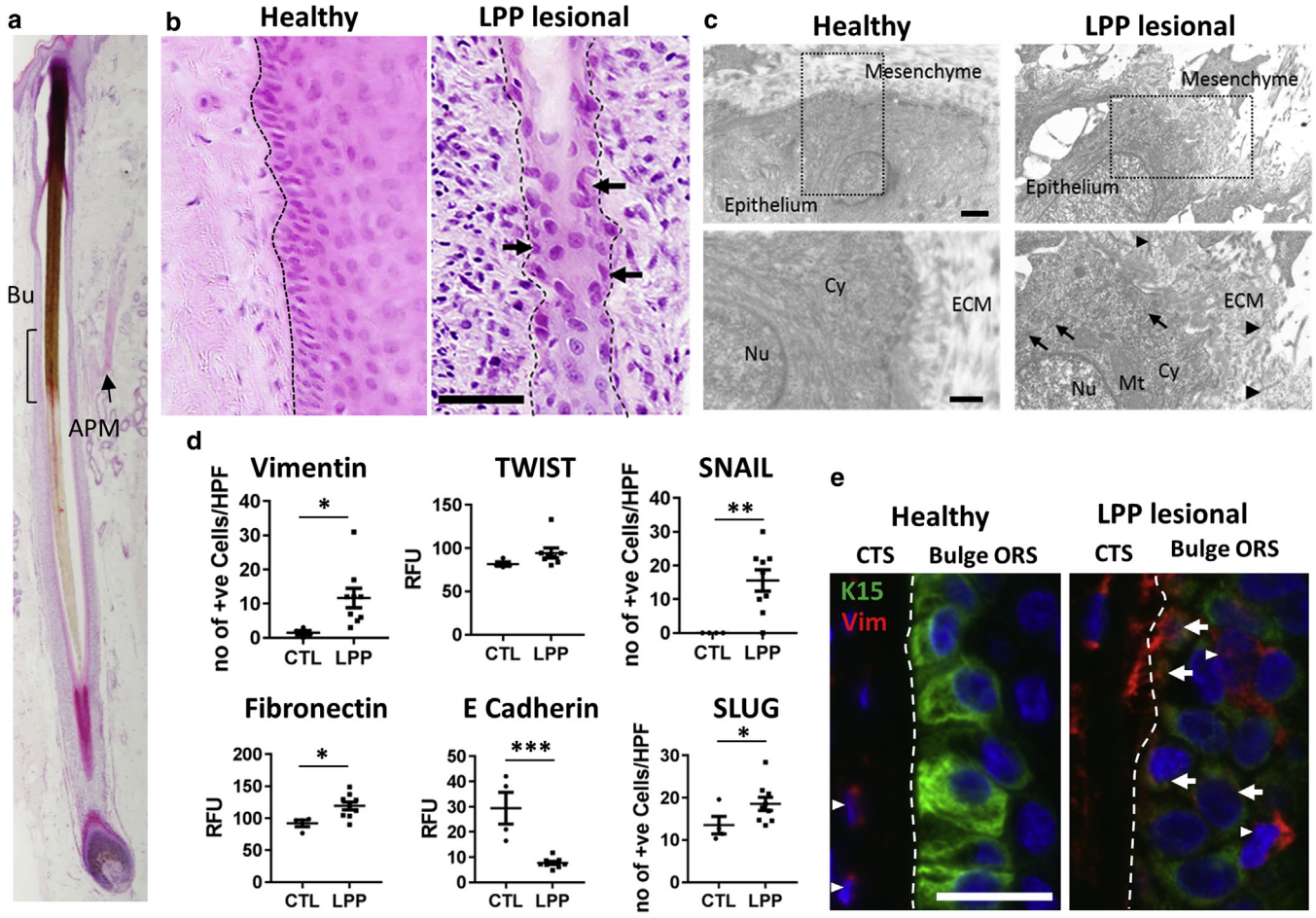

Figure 1. Evidence of epithelial-to-mesenchymal transition (EMT) can be identified within the bulge epithelium of lichen planopilaris (LPP) hair follicles (HFs). Hematoxylin and eosin histochemistry of a healthy human scalp HF indicating the bulge niche (**a**). Lesional LPP HFs display some cells with a spindled morphology within bulge epithelium (**b**). Transmission electron microscopy reveals that LPP bulge keratinocytes can be found with abnormal collagen fibers visible within their cytoplasm (**c**). Analysis of LPP tissue reveals changes in a panel of EMT-related markers (**d**). Co-expression of vimentin with the bulge epithelial stem cell (eSC) marker keratin 15 is observed (**e**). Black arrows in (**b**) denote cells of a fibroblast-like morphology. Arrows in (**c**) indicate intracellular collagen fibers, while arrowheads denote extracellular collagen fibers. White arrows in (**e**) identify cells double positive for vimentin and keratin 15 within the bulge, while arrowheads mark cells positive for vimentin alone. Boxes indicate areas of higher-power magnification, dashed lines indicate the basement membrane. Scale bar = 50 μm (**b**, **e**), 833 nm (**c**; upper panel), 500 nm (**c**; lower panel). $*P < 0.05$, $**P < 0.01$, $***P < 0.001$. APM, arrector pili muscle; Bu, bulge; CTL, control; CTS, connective tissue sheath; Cy, cytoplasm; ECM, extracellular matrix; Mt, mitochondria; Nu, nucleus; ORS, outer root sheath.

reduced in lesional LPP bulge epithelium (Harries et al., 2013). With patient biopsies, we are unable to conclusively prove the origin of these vimentin/keratin 15 double-positive cells. However, invasion of dermal fibroblasts into the bulge epithelium is, to our knowledge, previously unreported outside of malignancy, and we are not aware of any evidence that nonmalignant, nontransformed human mesenchymal cells (such as dermal fibroblasts) can ever express the eSC-associated keratin 15 in situ. Therefore, we conclude that the only plausible explanation for vimentin/keratin 15 double-positive cells is that eSCs underwent EMT within the bulge.

Our data clearly show that at least some human eSCs in the bulge epithelium of HFs affected by LPP undergo EMT, potentially contributing to the extensive scarring seen in LPP and likely other primary cicatrial alopecias. Therefore, future LPP management should also attempt to effectively inhibit the EMT of bulge eSCs before it becomes irreversible. Our findings are in line with the recent report that EMT also occurs in human HF epithelium in situ during keloid formation, as indicated by abnormal vimentin expression (Yan et al., 2015). Thus, it is conceivable that anti-EMT therapies developed by studying LPP as a model disease may also become applicable to other diseases characterized by excessive scar tissue formation.

EMT can be induced in healthy human HFs ex vivo

However, given that LPP is an orphan disease (ORPHA:525, http://www.orpha.net), clinical material is difficult to obtain, and patients typically only seek medical attention during late-stage disease (Sinclair, 2016). Therefore, we wondered whether it would be possible to experimentally mimic the early molecular changes associated with EMT in the bulge of microdissected, organ-cultured healthy human HFs (Langan et al., 2015).

We designed a cocktail of recognized EMT-promoting agents containing epidermal growth factor, transforming growth factor (TGF)-β1, IFN-γ, and the selective E-cadherin inhibiting peptide SWELYYPLRANL (peptide A) (Segal and Ward, 2017),

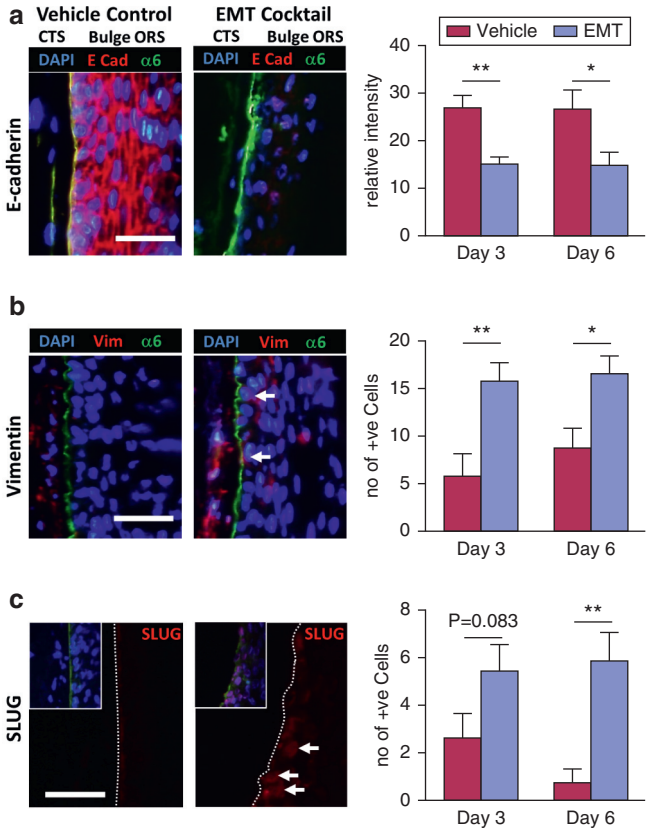

Figure 2. Bulge epithelial-to-mesenchymal transition (EMT) can be experimentally induced in healthy human hair follicles (HFs) ex vivo. HF organ cultures were prepared in the presence of an EMT-inducing cocktail (IFN-γ, transforming growth factor-β, epidermal growth factor, Peptide A; "EMT") or with vehicle alone as control (Veh). Figures show representative immunofluorescence images and quantification for E-cadherin (E-cad) (**a**) (red), vimentin (**b**) (red), and Slug (**c**) (red). Integrin α6 (green) was used to locate the basement membrane, which demarcates the borderline between bulge epithelium and its surrounding mesenchyme. Sections were counterstained with DAPI (blue). Data are presented as the mean of 3 independent experiments with full-length anagen VI scalp HFs from 3 different individuals (3 hair follicles per donor) ± standard error of mean. $^{*}P < 0.05$, $^{**}P < 0.01$. Scale bar = 50 μm. Arrows in (**b**) and (**c**) indicate positively labeled cells. CTS, connective tissue sheath; ORS, outer root sheath.

and exposed organ-cultured, full-length human anagen VI HFs that had been microdissected with their bulge area intact to this "EMT cocktail" (for details see Supplementary Methods online).

Intriguingly, after only 3 days, this rapidly, significantly, and reproducibly reduced E-cadherin transcript and protein expression in the bulge epithelium of EMT cocktail–treated HFs ex vivo compared to vehicle-treated control HFs (Figure 2a). Vice versa, vimentin and SLUG transcript and protein expression were significantly increased (Figure 2), replicating the changes observed in the bulge of lesional LPP. Extending the cultures to day 6 did not further increase these effects, suggesting that a maximal induction of EMT had occurred. Omitting any one of the EMT cocktails constituents reduced the potency of EMT induction (Supplementary Figure S3 online).

To our knowledge, this is the first report of both experimentally induced EMT in adult human eSCs within their physiological SC niche and in a healthy human (mini-)organ ex vivo. Given the critical importance of the eSC niche and its surrounding mesenchyme for HF development, growth, and survival (Sennett and Rendl, 2012), this simple but clinically relevant assay opens up new possibilities for interrogating and manipulating the obscure (patho-)biology of human eSCs that undergo EMT.

Moreover, as expected from the general EMT literature (Nieto et al., 2016; Pasquier et al., 2015; Serrano-Gomez et al., 2016; Stone et al., 2016, Zeisberg and Neilson, 2009), our assay identifies the suppression of E-cadherin–mediated signaling and stimulation by TGF-β1, epidermal growth factor, and IFN-γ as four molecular key signals sufficient to induce EMT in primary human eSCs in situ. This is well in line with the fact that TGF-β1 is typically overexpressed in fibrotic diseases (Walraven et al., 2017) and that IFN-γ is overexpressed in and around lesional LPP HFs (Harries et al., 2013). Therefore, our HF organ culture results encourage one to preferentially target these specific pathways in subsequent studies when attempting to therapeutically counteract EMT-related HF scarring and loss of eSCs.

Pioglitazone stimulates peroxisome proliferator–activated receptor-γ via downregulation of TGF-β, protecting against and partially reversing EMT induction

Next, we explored the utility of our new HF organ culture EMT assay for the identification of promising drugs that can counteract EMT in the eSC zone of human HFs. For this, we turned to the peroxisome proliferator–activated receptor (PPAR)-γ agonist, pioglitazone, which is a widely prescribed insulin-sensitizing agent primarily used for treating type 2 diabetes mellitus (DeFronzo et al., 2011). Pioglitazone reportedly can inhibit ocular EMT (Hatanaka et al., 2012). Compared to healthy skin, LPP skin shows a defect in PPAR-γ expression (Karnik et al., 2009), and PPAR-γ agonists have been advocated as a third-line therapy for LPP (Mirmirani and Karnik, 2009). Because PPAR-γ expression in the bulge itself does not differ between lesional and non-lesional LPP HFs (Harries et al., 2013), even diseased HFs should still be susceptible to PPAR-γ modulation.

HFs treated with the EMT cocktail only showed the expected EMT induction signature, namely, decreased E-cadherin alongside increased vimentin and SLUG expression ex vivo. However, when pioglitazone (30 μM) was administered to the culture medium 1 day before the EMT cocktail, E-cadherin and vimentin expression did not significantly differ from that of vehicle-treated control HFs (Figure 3a and Supplementary Figure S4 online). In addition, Slug protein expression was significantly reduced by pioglitazone pretreatment compared to EMT cocktail alone, although it was only partially repressed compared to vehicle treatment. The investigated pioglitazone dose was not capable of reversing the molecular EMT signature, when pioglitazone was added 72 hours after experimental EMT induction (Figure 3a).

Since epithelial cells grown in vitro readily adopt an EMT-like state (Stone et al., 2016), we also treated isolated HF keratinocytes from the outer root sheath in monolayer in order to explore the mechanism by which pioglitazone might inhibit EMT. After stimulation with pioglitazone, PPAR-γ was increased, while TGF-ß1, SMAD2, and SMAD3 mRNA expression was downregulated (Figure 3b). This effect was

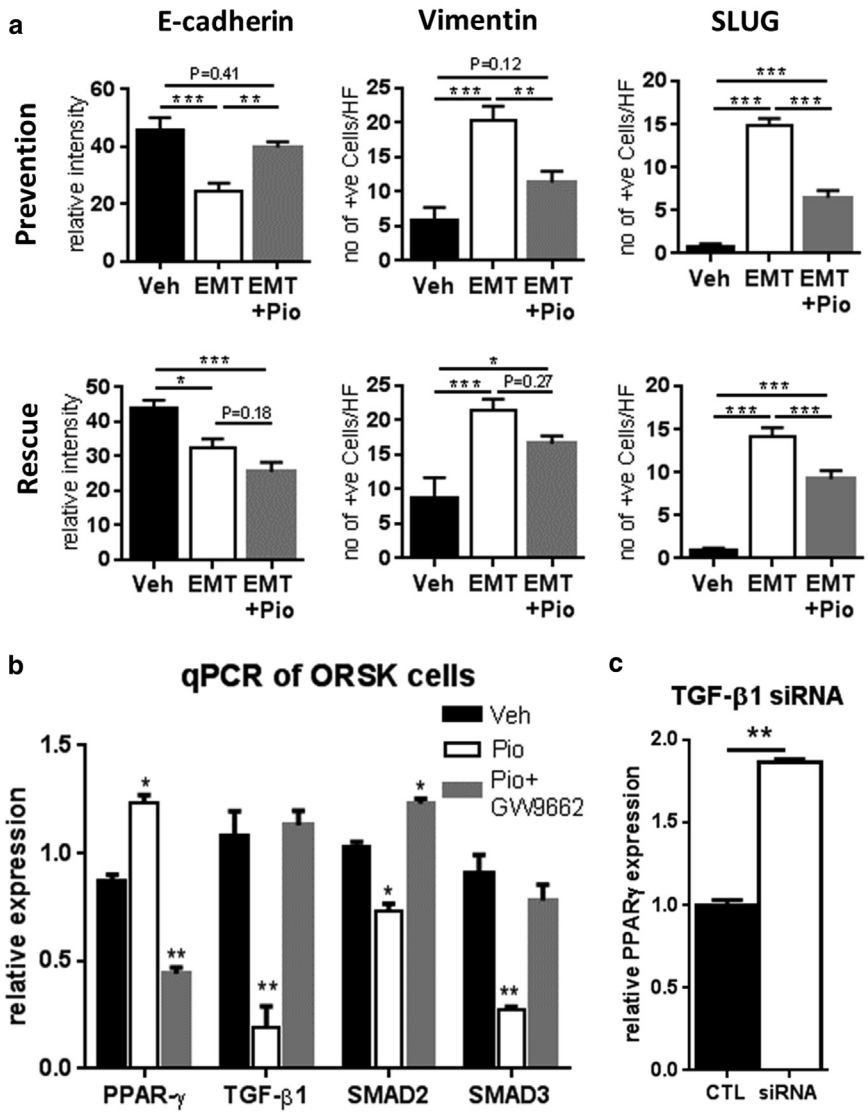

Figure 3. Peroxisome proliferator–activated receptor (PPAR)-γ stimulation by pioglitazone can partially repress induction of an epithelial-to-mesenchymal transition (EMT) signature, through inhibition of transforming growth factor (TGF)-β. The PPAR-γ agonist pioglitazone partially protected from EMT protein induction when treated 24 hours before the EMT-inducing cocktail, but did not reverse EMT when added 72 hours, retrospectively (**a**). Real-time quantitative PCR of human outer root sheath keratinocyte (ORSK) cells treated with pioglitazone reveals a suppression of expression of TGF-β pathway genes, which is blocked by the PPAR-γ antagonist GW9662 (**b**). PPAR-γ expression in ORSK cells is stimulated by knockdown of TGF-β1 by small interfering RNA (**c**). In (**a**) E-cadherin data are presented as the relative immunofluorescence intensity, while for SLUG and vimentin the numbers of positive cells per HF are shown. Data presented as the mean of 3 independent experiments ± standard error of mean, in (**a**) 3 HFs per donor (n = 9 HFs) Data in (**a**) and (**b**) were analyzed by analysis of variance, while data in (**c**) were analyzed by *t* test. $*P < 0.05$, $**P < 0.01$, $***P < 0.001$.

blocked by the co-treatment with the PPAR-γ antagonist GW9662 (Figure 3b). In addition, PPAR-γ stimulation was also enhanced when TGF-β1 expression was suppressed via small interfering RNA (Figure 3c). To further confirm this mechanism, we assessed paired lesional vs uninvolved whole-tissue biopsies from LPP patients. We found that TGF-β1, SMAD2, and SMAD3 transcripts were all upregulated, while PPAR-γ mRNA was downregulated (Supplementary Figure S5 online), adding further support for TGF-β signaling as a key mechanism for EMT in LPP, and underscoring the potential of PPAR-γ agonism in the treatment of this and perhaps other fibrotic diseases.

PPAR-γ stimulation by N-Acetyl-GED partially reverses EMT signature in normal and LPP HFs

Given that pioglitazone has adverse effects that question its utility for treating hair diseases (Ramot et al., 2015), we also investigated the EMT-modulatory activity of N-Acetyl-GED (AGED), a topically applicable PPAR-γ modulator that is undergoing clinical trials in acne vulgaris (PPM Services SA, 2017). This showed that all three tested concentrations of AGED significantly reduced the number of SLUG$^+$ or vimentin$^+$ cells compared to HFs treated with the EMT cocktail alone (Figure 4a and Supplementary Figure S6 online). Remarkably, this was seen when AGED was added either before (prevention) or after (rescue) EMT induction, suggesting that AGED may even be capable of partially reversing early-stage EMT.

However, AGED effects on bulge E-cadherin expression were unimpressive (Figure 4a). E-cadherin could not be rescued within the experimental window by either pioglitazone or AGED, suggesting that either the 3-day experimental window was insufficient to promote E-cadherin expression, or that additional signals are required to restore E-cadherin functionality. The lack of a dose-dependent response with AGED was surprising, although has been observed previously (Ramot et al., 2014). The reason for this might be due to measuring indirect effects of PPAR-γ activation or variability in the levels of EMT induced within each HF.

Finally, to understand whether AGED can reverse EMT in LPP, we collected fresh lesional biopsy material from two LPP patients. After 5 days, LPP skin organ-cultured under

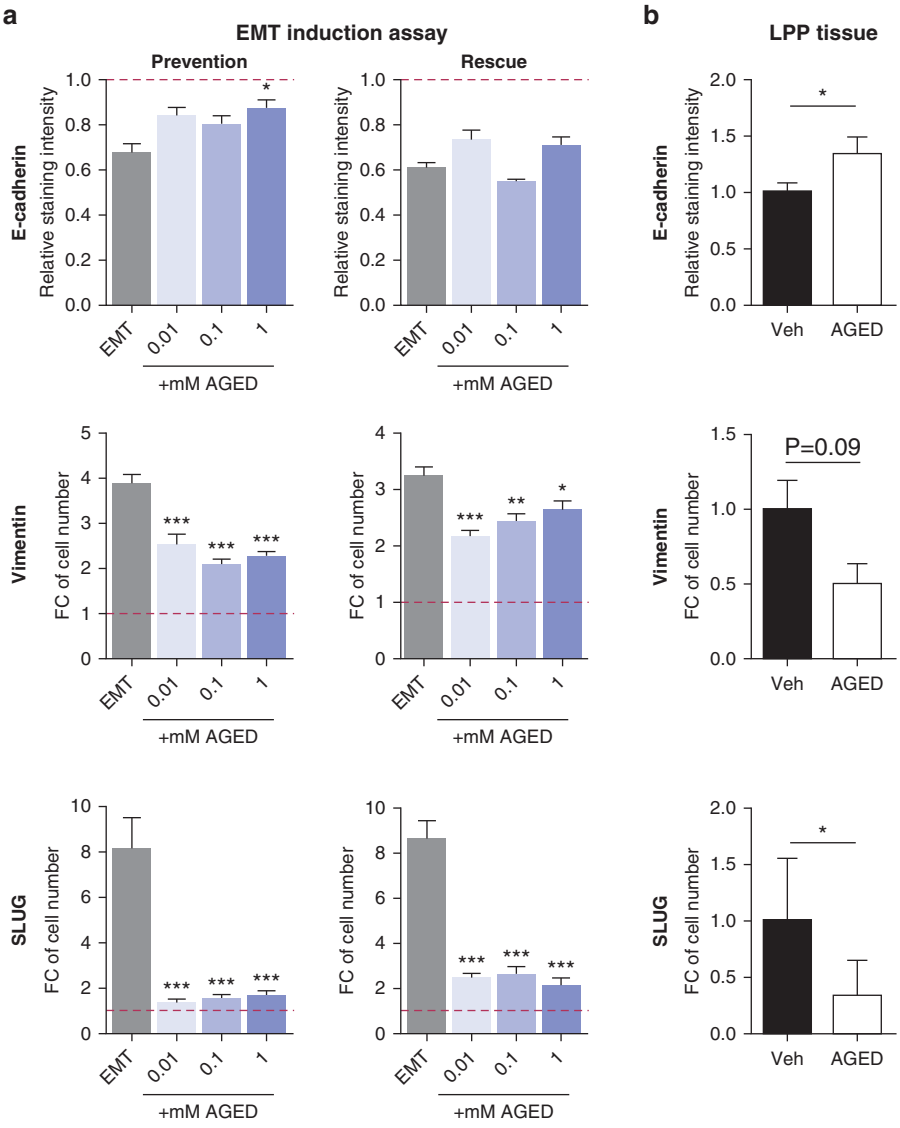

Figure 4. Peroxisome proliferator−activated receptor (PPAR)-γ stimulation by N-Acetyl-GED can partially rescue from an epithelial-to-mesenchymal transition (EMT) signature, in healthy and lichen planopilaris (LPP) hair follicles (HFs). The PPAR-γ agonist N-Acetyl-GED (AGED) not only protects against experimental EMT protein induction, but can also rescue SLUG expression to normal levels, and partially rescue vimentin expression (**a**). AGED significantly enhances E-cadherin expression and significantly inhibits SLUG expression in cultured LPP HFs, with a trend towards inhibition of vimentin (**b**). Data in (**a**) presented as mean values from 3 donors (n = 6−15 HFs per donor) normalized to vehicle-treated HFs and represented by a dotted line. Data in (**b**) presented as mean values normalized to vehicle control (veh) from 2 donors with n = 8−18 hair follicles per donor. Data in (**a**) were analyzed by analysis of variance, while data in (**b**) were analyzed by *t* test. E-cadherin are presented as the relative immunofluorescence intensity, while SLUG and vimentin data show the fold change (FC) difference in numbers of positive cells per HF. $^{*}P < 0.05$, $^{**}P < 0.01$, $^{***}P < 0.001$.

serum-free conditions (Harries et al., 2013) with 0.1 mM AGED showed a significant improvement in the protein expression of E-cadherin and SLUG the expression patterns of which tended toward that of healthy skin, while a nonsignificant trend was observed with vimentin (Figure 4b).

The reduction of experimentally induced EMT in the human bulge ex vivo with pioglitazone or AGED treatment demonstrates that our HF assay is well-suited as a screening system for identifying candidate drugs that may be repositioned for therapeutically counteracting EMT in human eSCs. Also, our results are well in line with evidence that PPAR-γ agonists attenuate experimentally induced fibrosis in other organs (Aoki et al., 2009; Ramot et al., 2015), possibly through the suppression of TGF-β signaling (Hatanaka et al., 2012). AGED is of particular interest in this context, because this PPAR-γ modulator may also protect human HF eSCs from apoptosis and stimulates keratin 15 expression in human scalp HF eSCs ex vivo (Ramot et al., 2014).

Given that LPP skin shows significantly reduced PPAR-γ transcription compared to healthy human scalp skin (Karnik et al., 2009) (Supplementary Figure S5), even though PPAR-γ expression does not differ significantly between lesional and non-lesional bulge epithelium in LPP patients (Harries et al., 2013), LPP patients may be at a disadvantage in suppressing EMT in their HF eSCs, before infiltration of $CD8^{+}$ T cells into the bulge (Figure 5). Thus, sufficient PPAR-γ−mediated signaling may well be critical for HF eSC maintenance and homeostasis, specifically in individuals predisposed to developing LPP. This further encourages one to systematically explore PPAR-γ modulators as complementary therapeutics in LPP (and other primary cicatrial alopecias) alongside immunosuppressive regimen. Reports of PPAR-γ agonist therapy in LPP are limited to small case series only; "improvement" (classified as a reduction in symptoms, diminished signs of inflammation, and cessation of hair loss progression) was reported in 50−70% cases, although complete remission was seen less frequently and scarring was not reversed (Baibergenova and Walsh 2012; Mesinkovska and Tellez, 2015; Mirmirani and Karnik 2009; Spring et al., 2013).

Moreover, as pioglitazone and AGED show slightly different efficiencies at inhibiting various EMT target genes, a combination of different PPAR-γ agonists might be used in

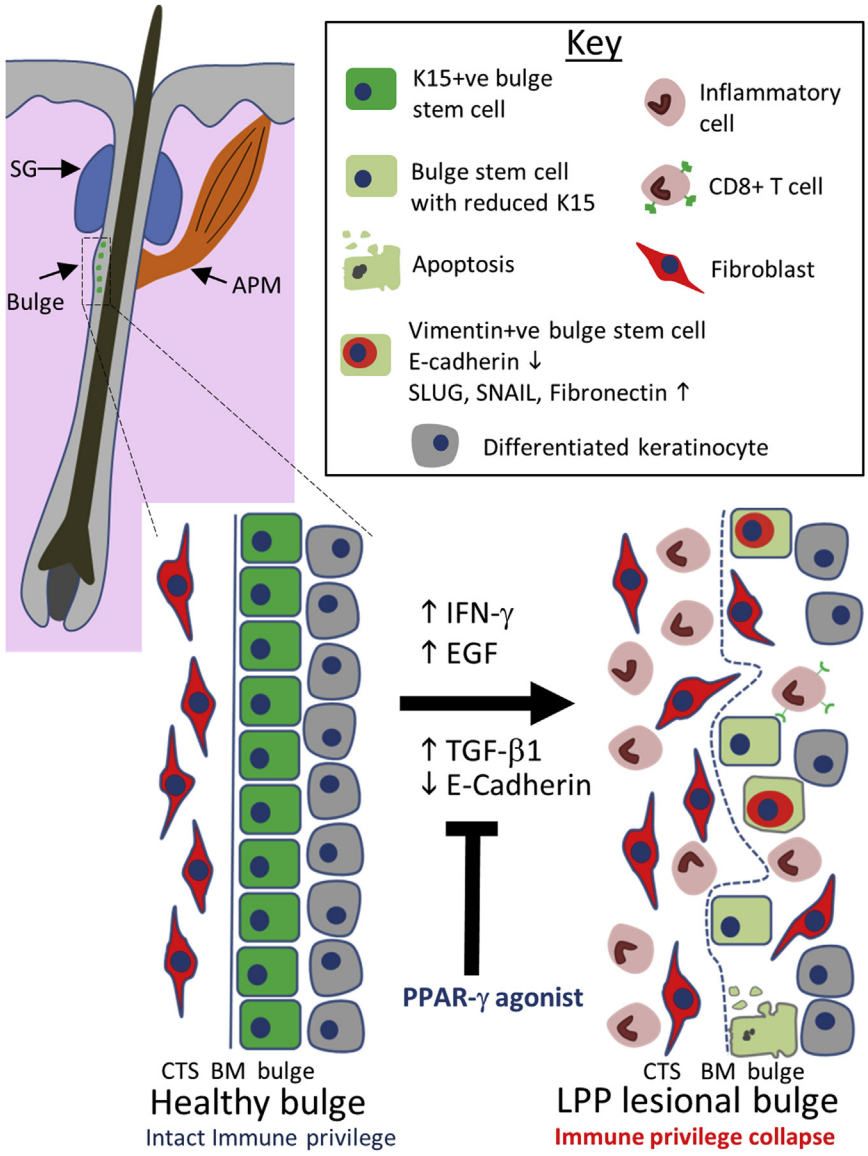

Figure 5. Proposed mechanism for lichen planopilaris development. Our available data suggest the following scenario: Inflammation- (T cell-?) induced downregulation of E-cadherin along with excessive IFN−γ, transforming growth factor-β (TGF-β), and epidermal growth factor (EGF) −signaling promote pathological EMT in bulge epithelial stem cells (eSCs) of human scalp HFs, thus contributing to the scarring associated with lichen planopilaris (LPP). Peroxisome proliferator−activated receptor (PPAR)-γ agonists may prevent or even partially reverse this EMT process, besides exerting eSC-protective and immunosuppressive functions, if administered early enough. APM, arrector pili muscle; BM, basement membrane; CTS, connective tissue sheath; SG, sebaceous gland.

concert to suppress EMT most effectively. Given its similarities to and differences from LPP, it will also be interesting to investigate next how AGED impacts on the extensive fibrosis seen in frontral fibrosing alopecia (Harries and Paus, 2010; Tzotzios et al., 2016; Jimenez et al., 2016).

In summary, our study introduces LPP as a model disease for pathological EMT in human adult eSCs, and shows that an EMT signature can be experimentally induced and therapeutically manipulated in these human eSCs within their niche, namely by PPAR-γ agonists.

MATERIALS AND METHODS

Study approval

LPP patient and health scalp tissue samples were obtained from the Manchester Skin Health Biobank (UK Ethics Committee approved study 14/NW/0185) at the University of Manchester, with additional samples from study 14/NW/0342. For experiments with AGED, healthy and LPP scalp tissue samples were obtained with ethical approval of the University of Las Palmas of Gran Canaria (CEIH-2014-06) or the University of Münster (2015-602-f-S). All samples were taken with informed patient consent.

Human tissue

Human scalp skin was obtained with written informed consent, with studies performed at the Salford Royal NHS Foundation Trust and University of Manchester. Diagnosis of LPP was determined via standard clinical and histopathological criteria (Harries et al., 2009; Sinclair, 2016). Many of the LPP specimens had been diagnostically classified and assessed during our previous study (Harries et al., 2013). Lesional specimens were taken from clinically inflamed edges of alopecia containing a reduced density of hairs and were fixed in formalin for paraffin embedding (for clinical features of each patient see Supplementary Table S2 online). Paired lesional and non-lesional specimens were also obtained from this cohort and snap-frozen in liquid nitrogen. Clinically healthy control samples (n = 4) were obtained from surplus occipital scalp skin of patients undergoing elective hair restoration surgery (mean age 50 years).

Quantitative real-time PCR

In order to permit optimal comparisons with the results from our previous study, the same RNA samples used previously (Harries et al., 2013) were used in the current study. Quantitative real-time PCR was performed on a StepOne Plus Real-Time PCR system using Taqman gene expression assays. Whole-tissue biopsies from paired lesion and uninvolved areas from three additional donors were used to profile TGF-β signaling, with RNA isolation and quantitative real-time PCR, as described previously (Panicker et al., 2012). For details of probes used, see Supplementary Table S3 online.

Human HF organ culture

Serum-free organ culture of human anagen scalp HFs was performed, as described previously (Langan et al., 2015), from the occipital or temporal scalp of patients undergoing hair-restoration surgery. Individual full-length HFs were dissected from the surrounding tissue or microdissected from the tissue and incubated overnight in culture media (Williams E media supplemented with insulin [10 μg/ml], hydrocortisone [40 ng/ml], L-glutamine [2 mM], penicillin [100 μg/ml], and streptomycin [100 U/ml]). The following day, HFs present in anagen VI were transferred to media supplemented with either vehicle or a cocktail of agents known to promote EMT (i.e., TGF-β1 [3 ng/ml], epidermal growth factor [10 ng/ml], and IFN-γ [500 IU/ml]) or to inhibit E-cadherin–mediated cell-to-cell contact (H-SWELYYPLRANL-NH2; Peptide A, 500 nM [Segal and Ward, 2017]). HFs were harvested into OCT embedding compound and stored at −80°C before use. In co-culture studies, pioglitazone (30 μM; Enzo Life Sciences, Farmingdale, NY) or AGED (0.01, 0.1, 1 mM; PPM Services SA, Ticino, Switzerland) was added either 24 hours before (prevention) or 72 hours after (rescue) addition of the EMT cocktail.

Culture of LPP tissue

A single 4-mm punch was taken from lesional LPP skin of two female donors (44 and 78 years old). The biopsy was cut in half with each piece of tissue grown in culture media (Harries et al., 2013). Tissue was dosed with vehicle or 0.1 mM AGED on days 1 and 3, with the tissue harvested at day 5 and snap-frozen in Cryomatrix (Thermo Fisher, Waltham, MA).

Culture of human outer root sheath keratinocyte cells

Primary human HF outer root sheath cells were purchased from ScieCell Research Labs (Carlsbad, CA) and cultured as described previously (Panicker et al., 2012). Cells at passage 3 or 4 were seeded at 0.6×10^6 cells per well and treated with 10 μM pioglitazone, 10 μM pioglitazone plus 10 μM GW9662 (Cayman Chemicals, Ann Arbor, MI), or vehicle for 16–24 hours. Data are taken from three independent experiments and analyzed using one-way analysis of variance.

TGF-β1 small interfering RNA (50 μM) was added to outer root sheath keratinocyte cells for 24 hours compared to empty vector alone (OriGene, Rockville, MD).

Immunohistochemistry and quantitative immunohistomorphometry

Six-micrometer sections were used for immunohistochemistry of fixed in formalin for paraffin embedding and frozen samples. Heat-induced antigen retrieval (citrate or Tris-EDTA) was performed as required. For immunohistochemical protocol summary, see Supplementary Table S4 online. Immunostaining intensity of the HF bulge was assessed by quantitative immunohistomorphometry using ImageJ software (National Institutes of Health, Bethesda, MD), as described previously (Harries et al., 2013). Only HFs where the bulge region could be definitively identified were used for analysis; for biopsy samples this was confirmed by positioning of the arrector pili muscle, and for organ cultured HFs the co-localization with α6 integrin was used to mark the basement membrane. For the AGED experiments, vimentin, SLUG, and E-cadherin immunoreactivity was evaluated in 9–12 HFs/donor in three independent experiments (three different donors) for the rescue or prevention assay. For this assays, pooled data from three donors are presented as fold increase of mean ± standard error of mean. Statistical analysis was performed using Mann-Whitney and $P < 0.05$ was considered as significant.

Transmission electron microscopy

Samples were prefixed with 2.5% glutaraldehyde and 2% paraformaldehyde in 0.1 M phosphate buffer and fixed with 1% osmium tetroxide in the same buffer. Samples were then dehydrated via ethanol gradient, immersed in propylene oxide, and embedded in resin. Ultrathin sections were stained with tannic acid-uranyl acetate solution and lead citrate, and observed using the H-7500 apparatus (Hitachi, Japan).

Statistics

Nonpaired samples were compared using two-sample Student *t* test assuming equal or unequal variance after *F* test. Human HF organ culture groups were compared using one-way analysis of variance. For the AGED human HF organ culture, pooled data from three donors are presented as fold-change compared to vehicle and analyzed by Mann-Whitney test. Data are expressed as mean ± standard error of mean; *P* values < 0.05 were deemed significant.

CONFLICT OF INTEREST

Monasterium Laboratory received industry funding for testing AGED ex vivo (see Acknowledgments). JC is an employee of Monasterium Laboratory, while MB (CSO) and RP (Founder) serve as consultants for Monasterium Laboratory.

ACKNOWLEDGMENTS

The authors gratefully acknowledge Akiko Imanishi, Weiping Li, Francesco Bozza, Stella Pearson, Nathan Hawkshaw, Derek Pye, Nur Azida Nasir, and Janine Jakobs for technical assistance. The authors also gratefully acknowledge Pratima Karnik, in whose laboratory and under whose supervision SP generated the data shown in Figures 3 and Supplementary Figure 5 during his time as post-doctoral research fellow with Pratima Karnik. Daisuke Tsuruta is acknowledged for his overall support and collaboration. Work was funded in part by grants from the Cicatricial Alopecia Research Foundation and the British Skin Foundation to RP and MH, by PPM Services S.A, Morbio Inferiore/CH. for N-Acetyl-GED–related research to Monasterium Laboratory, and by the National Institute for Health Research Biomedical Research Centre, Manchester, to RP.

AUTHOR CONTRIBUTIONS

The study was conceived and supervised by RP, and the experiments were devised by HI, DA, CW, and RP; experimental work was conducted by HI, DA, JC, MH, TB, EP, FJ, JH, and SP; data analysis was performed by HI, DA, MH, JC, MB, TB, NS, EP, JH, and CW. The manuscript was written by HI, DA, and RP. All authors edited the manuscript, and approve the final version.

SUPPLEMENTARY MATERIAL

Supplementary material is linked to the online version of the paper at www.jidonline.org, and at https://doi.org/10.1016/j.jid.2017.09.047.

REFERENCES

Aoki Y, Maeno T, Aoyagi K, Ueno M, Aoki F, Aoki N, et al. Pioglitazone, a peroxisome proliferator-activated receptor gamma ligand, suppresses bleomycin-induced acute lung injury and fibrosis. Respiration 2009;77:311–9.

Baibergenova A, Walsh S. Use of pioglitazone in patients with lichen planopilaris. J Cutan Med Surg 2012;16:97–100.

DeFronzo RA, Tripathy D, Schwenke DC, Banerji M, Bray GA, Buchanan TA, et al. Pioglitazone for diabetes prevention in impaired glucose tolerance. N Engl J Med 2011;364:1104–15.

Dubois-Marshall S, Thomas JS, Faratian D, Harrison DJ, Katz E. Two possible mechanisms of epithelial to mesenchymal transition in invasive ductal breast cancer. Clin Exp Metastasis 2011;28:811–8.

Harries MJ, Meyer K, Chaudhry I, J EK, Poblet E, Griffiths CE, et al. Lichen planopilaris is characterized by immune privilege collapse of the hair follicle's epithelial stem cell niche. J Pathol 2013;231: 236–47.

Harries MJ, Paus R. The pathogenesis of primary cicatricial alopecias. Am J Pathol 2010;177:2152–62.

Harries MJ, Trueb RM, Tosti A, Messenger AG, Chaudhry I, Whiting DA, et al. How not to get scar(r)ed: pointers to the correct diagnosis in patients with suspected primary cicatricial alopecia. Br J Dermatol 2009;160:482–501.

Hatanaka H, Koizumi N, Okumura N, Kay EP, Mizuhara E, Hamuro J, et al. Epithelial-mesenchymal transition-like phenotypic changes of retinal pigment epithelium induced by TGF-beta are prevented by PPAR-gamma agonists. Invest Ophthalmol Vis Sci 2012;53:6955–63.

Ito M, Liu Y, Yang Z, Nguyen J, Liang F, Morris RJ, et al. Stem cells in the hair follicle bulge contribute to wound repair but not to homeostasis of the epidermis. Nat Med 2005;11:1351–4.

Jethwa P, Naqvi M, Hardy RG, Hotchin NA, Roberts S, Spychal R, et al. Overexpression of Slug is associated with malignant progression of esophageal adenocarcinoma. World J Gastroenterol 2008;14:1044–52.

Jimenez F, Harries M, Poblet E. Frontal fibrosing alopecia: a disease fascinating for the researcher, disappointing for the clinician and distressing for the patient. Exp Dermatol 2016;25:853–4.

Karnik P, Tekeste Z, McCormick TS, Gilliam AC, Price VH, Cooper KD, et al. Hair follicle stem cell-specific PPARgamma deletion causes scarring alopecia. J Invest Dermatol 2009;129:1243–57.

Langan EA, Philpott MP, Kloepper JE, Paus R. Human hair follicle organ culture: theory, application and perspectives. Exp Dermatol 2015;24:903–11.

Mesinkovska NA, Tellez A, Dawes D, Piliang M, Bergfeld W. The use of oral pioglitazone in the treatment of lichen planopilaris. J Am Acad Dermatol 2015;72:355–6.

Mirmirani P, Karnik P. Lichen planopilaris treated with a peroxisome proliferator-activated receptor gamma agonist. Arch Dermatol 2009;145: 1363–6.

Nakamura M, Tokura Y. Epithelial-mesenchymal transition in the skin. J Dermatol Sci 2011;61:7–13.

Nakamura M, Tokura Y. Expression of Snail1 in the fibrotic dermis of postmenopausal frontal fibrosing alopecia: possible involvement of an epithelial-mesenchymal transition and a review of the Japanese patients. Br J Dermatol 2010;162:1152–4.

Nieto MA, Huang RY, Jackson RA, Thiery JP. EMT: 2016. Cell 2016;166: 21–45.

Ogawa Y, Shimmura S, Kawakita T, Yoshida S, Kawakami Y, Tsubota K. Epithelial mesenchymal transition in human ocular chronic graft-versus-host disease. Am J Pathol 2009;175:2372–81.

Panicker SP, Ganguly T, Consolo M, Price V, Mirmirani P, Honda K, et al. Sterol intermediates of cholesterol biosynthesis inhibit hair growth and trigger an innate immune response in cicatricial alopecia. PLoS One 2012;7:e38449.

Pasquier J, Abu-Kaoud N, Al Thani H, Rafii A. Epithelial to mesenchymal transition in a clinical perspective. J Oncol 2015;2015:792182.

PPM Services SA. A double-blind, randomised, placebo-controlled clinical study to evaluate the efficacy and safety of N-Acetyl-GED-0507-34-LEVO gel, 1 and 2%, applied once daily for 12 weeks in patients with mild to moderate facial acne vulgaris. www.clinicaltrialsregister.eu/ctr-search/trial/2016-000540-33/HU. Accessed February 17, 2017.

Purba TS, Haslam IS, Poblet E, Jimenez F, Gandarillas A, Izeta A, et al. Human epithelial hair follicle stem cells and their progeny: current state of knowledge, the widening gap in translational research and future challenges. Bioessays 2014;36:513–25.

Ramot Y, Mastrofrancesco A, Camera E, Desreumaux P, Paus R, Picardo M. The role of PPARgamma-mediated signalling in skin biology and pathology: new targets and opportunities for clinical dermatology. Exp Dermatol 2015;24:245–51.

Ramot Y, Mastrofrancesco A, Herczeg-Lisztes E, Biro T, Picardo M, Kloepper JE, et al. Advanced inhibition of undesired human hair growth by PPARgamma modulation? J Invest Dermatol 2014;134:1128–31.

Segal JM, Ward CM. Novel peptides for deciphering structural and signalling functions of E-cadherin in mouse embryonic stem cells. Sci Rep 2017;7: 41827.

Sennett R, Rendl M. Mesenchymal-epithelial interactions during hair follicle morphogenesis and cycling. Semin Cell Dev Biol 2012;23:917–27.

Serrano-Gomez SJ, Maziveyi M, Alahari SK. Regulation of epithelial-mesenchymal transition through epigenetic and post-translational modifications. Mol Cancer 2016;15:18.

Siar CH, Ng KH. Differential expression of transcription factors Snail, Slug, SIP1, and Twist in ameloblastoma. J Oral Pathol Med 2014;43:45–52.

Sinclair R. Scarring disorders of hair growth. In: Griffiths C, Barker J, Bleiker T, Chalmers R, Creamer D, editors. Rook's Textbook of Dermatology. 9th ed. Oxford: Wiley/Blackwell; 2016:89.34–44.

Spring P, Spanou Z, de Viragh PA. Lichen planopilaris treated by the peroxisome proliferator activated receptor-gamma agonist pioglitazone: lack of lasting improvement or cure in the majority of patients. J Am Acad Dermatol 2013;69:830–2.

Stone RC, Pastar I, Ojeh N, Chen V, Liu S, Garzon KI, et al. Epithelial-mesenchymal transition in tissue repair and fibrosis. Cell Tissue Res 2016;365:495–506.

Szabo AZ, Fong S, Yue L, Zhang K, Strachan LR, Scalapino K, et al. The CD44+ ALDH+ population of human keratinocytes is enriched for epidermal stem cells with long-term repopulating ability. Stem Cells 2013;31:786–99.

Tziotzios C, Stefanato CM, Fenton DA, Simpson MA, McGrath JA. Frontal fibrosing alopecia: reflections and hypotheses on aetiology and pathogenesis. Exp Dermatol 2016;25:847–52.

Walraven M, Akershoek JJ, Beelen RH, Ulrich MM. In vitro cultured fetal fibroblasts have myofibroblast-associated characteristics and produce a fibrotic-like environment upon stimulation with TGF-beta1: is there a thin line between fetal scarless healing and fibrosis? Arch Dermatol Res 2017;309:111–21.

Yan L, Cao R, Wang L, Liu Y, Pan B, Yin Y, et al. Epithelial-mesenchymal transition in keloid tissues and TGF-beta1-induced hair follicle outer root sheath keratinocytes. Wound Repair Regen 2015;23:601–10.

Zeisberg M, Neilson EG. Biomarkers for epithelial-mesenchymal transitions. J Clin Invest 2009;119:1429–37.